Rare Metal Materials and Engineering
Volume 52, Issue 12, December 2023
Available online at www.rmme.ac.cn

Science Press

Cite this article as: Sun Wanshuo, Cheng Junsheng, Wang Lei, et al. Preparation of Nb_3Sn-NbTi Hybrid Superconducting Joint by Resistive Welding Technique[J]. Rare Metal Materials and Engineering, 2023, 52(12): 4040-4046. DOI: 10.12442/j.issn.1002-185X.20230493.

ARTICLE

Preparation of Nb_3Sn-NbTi Hybrid Superconducting Joint by Resistive Welding Technique

Sun Wanshuo[1,2], Cheng Junsheng[1,2,3], Wang Lei[1,2,3], Chen Shunzhong[1,2], Guo Qiang[4]

[1] Institute of Electrical Engineering, Chinese Academy of Sciences, Beijing 100190, China; [2] University of Chinese Academy of Sciences, Beijing 100049, China; [3] Institute of Electrical Engineering and Advanced Electromagnetic Drive Technology, Jinan 250102, China; [4] Western Superconducting Technologies Co., Ltd, Xi'an 710018, China

Abstract: In high magnetic field magnets, especially those with high stability requirements, superconducting joints with ultra-low resistances play an important role in magnet fabrication. The Nb_3Sn and NbTi joints were fabricated by the resistive welding technique. The Nb_3Sn joint was fabricated by sintering the Nb-Sn precursors after mechanical alloying. Then the Nb_3Sn bulk in the Nb_3Sn joint was welded to the NbTi conductor. The microstructure and grain sizes of Nb_3Sn bulk after long periods of time at high temperature were investigated. After welding, the joint was analyzed using X-ray nano-CT technology to display the connecting status and the defects between the Nb_3Sn and NbTi conductor without destroying the joint. The electrical characteristics of the joints were measured under background fields through the field decay method. Results show that compared with the ones prepared by the commonly used solid matrix replacement technique, the prepared joint exhibits better magnetic field resistance and lower resistance at 1.5 T background field.

Key words: Nb_3Sn conductor; NbTi conductor; superconducting joints

Superconducting joint is one of the most important components in the magnet system because superconducting wires are not long enough to wound the whole magnet due to limitations of process conditions. Typically, a superconducting magnet consists of several joints of the same (NbTi to NbTi, Nb_3Sn to Nb_3Sn) and different materials (Nb_3Sn to NbTi). For large scale magnets, the numbers of joints reach dozens or even hundreds. The joints have different physical and chemical properties of the original materials, which results in joint resistance. The superconducting current flowing in the magnet generates loss when passing through joints and generates heat in joints, which causes further deterioration in the cooling operating environment. The superconducting joint significantly influences the magnet operation, especially for a high stability magnet operated in a closed loop mode. Every superconducting joint resistance and their sum in the magnet must be low enough to meet the requirements of current decay rate.

Two of the most commonly used low-temperature superconducting materials are Nb_3Sn and NbTi. Nb_3Sn has a A-15 intermetallic structure and can be fabricated either above 930 °C in the presence of a Nb-Sn melt or by solid state reactions[1]. NbTi is a kind of alloy with a dominant position in superconducting magnet market due to its ductile properties and low cost[2]. These two superconducting materials have been widely used in many fields, such as magnetic resonance imaging (MRI)[3], nuclear magnetic resonance (NMR), fusion program such as International Thermonuclear Experiment Reactor[4] and other high-field magnets. Typically, a magnet above 10 T uses both NbTi and Nb_3Sn coils to provide a central magnetic field. The two types of coils work within their respective ranges of field to maximize their efficiencies. Thus, superconducting joints are needed to connect the NbTi and Nb_3Sn coils. In addition, several Nb_3Sn magnets consist of several coils. The joints of NbTi and Nb_3Sn wires are also suitable to the Nb_3Sn magnets, including several coils in different formers. A few Nb_3Sn magnets are made of different types of Nb_3Sn wires and need to be heat-treated under

Received date: August 08, 2023
Foundation item: National Key R&D Program of China (2022YFB3804004, 2022YFF0706904); National Natural Science Foundation of China (52307032)
Corresponding author: Cheng Junsheng, Ph. D, Professor, Institute of Electrical Engineering, Chinese Academy of Sciences, Beijing 100190, P. R. China, Tel: 0086-10-82547259, E-mail: jscheng@mail.iee.ac.cn

different schedules. As such, the Nb_3Sn magnet cannot be operated manually after heat-treatment due to the fragility of the A-15 superconducting phases.

Various methods have been proposed for fabricating the superconducting joints such as solid matrix replacement[5], cold-pressing technique[6-7], electromagnetic forming method[8], and ultrasonic welding[9]. All of these methods are used to fabricate the NbTi superconducting joints because of its alloy with high plasticity and machinability, but most of them are not suitable for Nb_3Sn joints due to the brittleness mentioned above. The solid matrix replacement method can be applied for fabricating the Nb_3Sn and NbTi joints. Superconducting solders are used as medium to connect the current between Nb_3Sn and NbTi conductors. However, these joints cannot work in high magnetic field under 1.5 T, and usually, its application range is lower than 0.5 T background field considering the safety of the magnet system[8]. Nb_3Sn-friendly methods are needed to fabricate the superconducting joints involved in Nb_3Sn conductors.

In this study, the resistive welding technique was applied to the Nb_3Sn and NbTi superconducting joints. Using this method, Nb_3Sn wires can be connected with NbTi wires, providing more convenience and flexibility of NbTi material. The Nb_3Sn and NbTi superconducting joints with ultra-low resistance were fabricated by the method and the obtained joins can work in high magnetic field above 1.5 T.

1 Experiment

1.1 Preparation of Nb_3Sn and NbTi joint

The ends of the Nb_3Sn wires were immersed in nitric acid to remove their stable outer layers. The exposed filaments were then immersed in a mixed acid solution to etch the surfaces, and then cleaned by water and alcohol in sequence. The loose filaments were twisted to increase their contact areas and the reliability of the joint. Using a high energy mechanical alloying method, the Nb and Sn powders with a stoichiometric ratio of 3:1 were blended and alloyed to form the Nb-Sn precursors. The ends of the Nb_3Sn wires were inserted into a mold that can join the filaments with the Nb-Sn precursors. Through the mold, the Nb_3Sn wires and the Nb-Sn precursors were pressed into a block. Similarly, the other ends of the Nb_3Sn wires were fabricated into another block. Then, the Nb_3Sn wires with two blocks on their two ends were heat treated in the furnace. We adopted a heat treatment schedule the same as that for the original wire. The five dwell stages were 210 °C for 100 h, 340 °C for 50 h, 450 °C for 50 h, 575 °C for 100 h, and 650 °C for 150 h. After heat treatment, the Nb_3Sn wires were connected with two Nb_3Sn bulks on both ends. Due to its high plasticity, NbTi superconducting wire is more easily manipulated compared with Nb_3Sn. The copper layer on the NbTi wires was removed by nitric acid to expose the NbTi filaments. Similarly, the NbTi filaments were etched and cleaned. The NbTi filaments were welded together with the Nb_3Sn bulk through resistive welding technology. The current capacity was 10−20 A. Six spots were welded on both joints of NbTi and Nb_3Sn.

1.2 Analysis

The microstructure was characterized by scanning electron microscopy (SEM) and the sample composition was identified by energy dispersive spectroscopy (EDS) system. Phase identification of the samples was characterized by X-ray diffraction (XRD, Bruker D8 Advance) with Cu Kα radiation. The grain orientations and phase maps of the sample were examined by electron backscatter diffraction (EBSD). The sample plane was defined as the RD-TD plane (RD: roll direction; TD: transverse direction). ND (normal direction) was the direction perpendicular to the RD-TD plane. The Nb_3Sn bulk after heat treatment at 650 °C for 150 h processed by focused ion beam (FIB) technique was submitted to transmission electron microscopy (TEM) examination. X-ray 3D computed tomography (CT) was utilized to characterize the connecting status and internal defects of the Nb_3Sn-NbTi joints. The superconducting property of the sample was examined by a physical property measurement system (PPMS) up to 9 T. The T_c value was determined by choosing the first deviation point from linearity that signifies the transition from normal to superconducting state. The Nb_3Sn-NbTi joint resistance was tested using the resistance measuring device based on the current decay method. The joint was immersed in liquid helium to achieve the superconducting state.

2 Results and Discussion

Fig.1 shows the SEM image and EDS mappings of the Nb-Sn powders after mechanical alloying of 5 h. Subsequently, the alloying product generates agglomeration, forming large particles, which are made of ultra-fine particles by the reaction of surface energy. As seen in Fig.1b and 1c, Nb and Sn elements are uniformly distributed and overlay the outline of the particles. Given the size of 5−15 μm in diameter for original powders, the Nb and Sn powders are milled into the Nb-Sn compounds with ultra-fine sizes and mixed with a stoichiometric ratio of microscopic constituent elements, which has a significant effect on the following solid-state diffusion reaction due to the shorter diffusion distance of Nb and Sn.

Fig.2a shows the typical SEM image of the Nb-Sn powders after mechanical alloying for 5 h. The image reveals that the Nb-Sn powders show flake structures that envelop each other. After heat treatment, the Nb-Sn powders react to form Nb_3Sn product with dense structure and small grain sizes, as seen in Fig.2b.

The XRD pattern of the obtained Nb_3Sn bulk heat treated at 650 °C for 150 h shows that most of peaks can be indexed to the Nb_3Sn structure (Fig. 3a). This result indicates that an almost single-phase Nb_3Sn phase has been synthesized. The compounds of Nb and Sn after ball-milling react to form Nb_3Sn without impurities such as the reactant and the intermediate products of the preparation. The sintered bulk is also confirmed by the temperature dependence of the DC susceptibility (Fig. 3b). The onset T_c of the sample is appro-

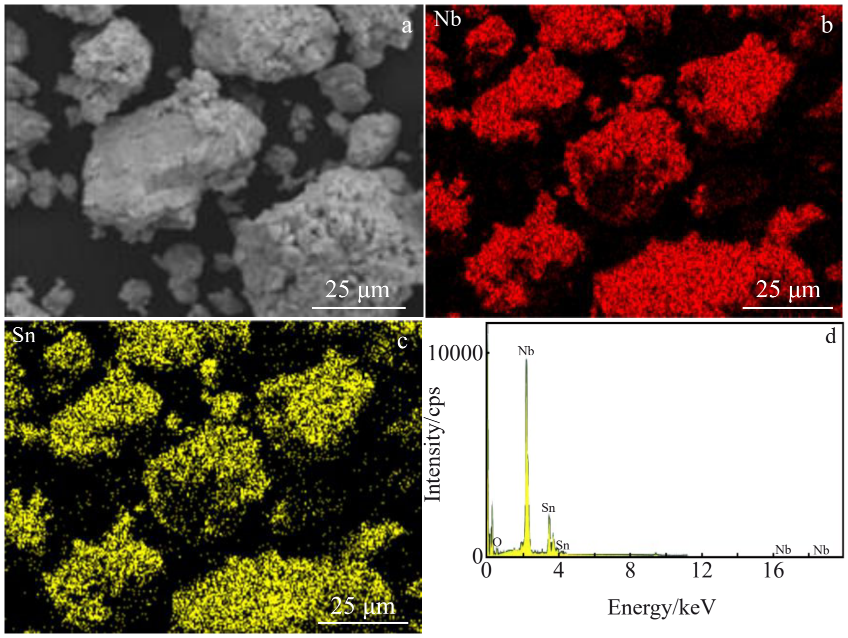

Fig.1 SEM image (a) and EDS results (b–d) of Nb-Sn powders with a ratio of 3:1 after mechanical alloying of 5 h

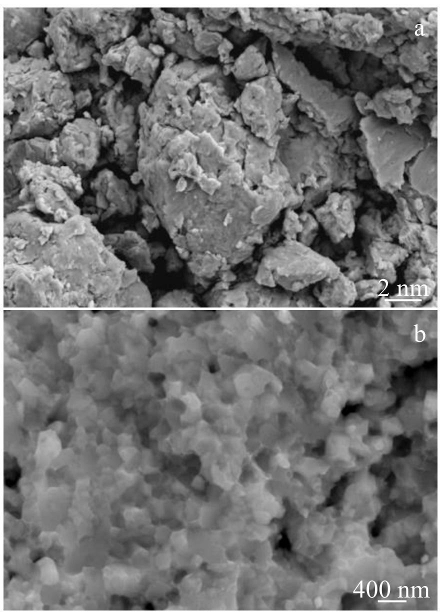

Fig.2 SEM images of the samples after mechanical alloying (a) and heat treatment (b)

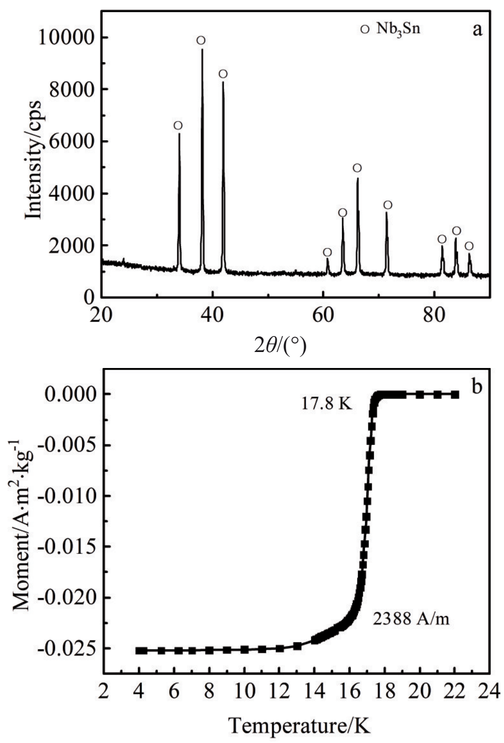

Fig.3 XRD pattern of the bulk sample after heat treatment (a) and temperature dependence of the DC magnetic susceptibility curve in an applied field of 2388 A/m (b)

ximately 17.8 K. The temperature-independent magnetic moment at low temperatures (below 10 K) suggests that no Nb reactants left. The sharp superconducting transition indicates a high electromagnetic homogeneity of the sintered Nb_3Sn bulk.

Fig.4 shows the EBSD results of the sample heat treated at 650 °C for 150 h, which is a commonly used schedule for Nb_3Sn superconducting wires. However, such a long heat treatment time is unknown for the precursors after mechanical alloying. We carried out the experiment to test if the long periods of time at high temperature of 650 °C results in excessive grain growth and affect the grain orientations. In previous literature in 2021[10], the Nb_3Sn formation reaction is driven for only a short time (24 h) for the precursors after mechanical alloying. The phase map in the figure shows that the Nb_3Sn phases (in yellow) are formed and uniformly distributed in the sample. Several areas that are not indexed might be attributed to the difficulties of sample preparations

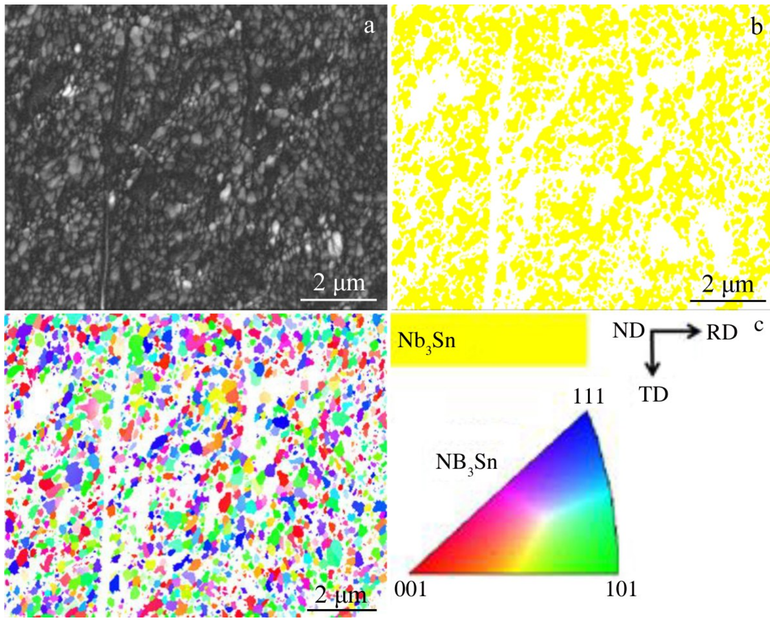

Fig.4 EBSD results of the sample heat treated at 650 °C for 15 h: (a) band contrast map, (b) phase map, and (c) grain orientation map in ND for EBSD measurement.

The grain orientation map in ND indicates that the Nb_3Sn grains have random orientations. The Nb_3Sn grains have almost the same growth velocity, and equiaxed grains with crystallizing morphology. The small sizes of the Nb_3Sn grains indicate that the grain growth is not severely affected by the long periods of time at high temperatures. After mechanical alloying, nanocrystalline grains are formed and have finer grain sizes and large amounts of boundaries that provide many evenly distributed nucleation sites. In addition, Nb and Sn atoms are uniformly mixed with 3: 1 stoichiometry on the microscale.

Fig.5 shows the pole and inverse pole figures of the sample heat treated at 650 °C for 150 h. The results indicate that the Nb_3Sn grains have no apparent textures but can be described by the orientation of {133} <103> and <112> . These orientations might be related to that of the original Nb.

To further investigate the microstructure of the Nb_3Sn joint, the Nb_3Sn bulk was subjected to TEM examination. The grain size of Nb_3Sn has a significant influence on the superconducting properties of Nb_3Sn conductors. Fine Nb_3Sn grains produce a high density of grain boundaries, which can act as pinning on the centers of the flux and improve the critical current density[11–12]. An elevated temperature heat treatment for long periods of time usually results in the increase in grain size for most materials. The investigations of the sample after the long periods of time (150 h) at high temperature of 650 °C show that the grain size dispersion ranges within 50–200 nm. Fig. 6a shows that the results are consistent with the EBSD result above, indicating no grain overgrowth. Fig. 6b displays the overlays of the TEM image and EDS maps of Nb and Sn elements, which are uniformly distributed in the sample with no enrichment of elements. The good homogeneity of the sample is further confirmed by EDS mapping (Fig. 6c), indicating that the Nb_3Sn phases are homogeneously distributed.

Fig.7 clearly shows the Nb_3Sn grains and clean boundaries. With selected area electron diffraction (SAED), we confirm the Nb_3Sn phase based on the crystal plane spacing and the angle of the crystal planes. Fig. 7c and 7d show the high-resolution TEM (HRTEM) images of the adjacent grains. TEM investigations reveal the formation of Nb_3Sn and the grain sizes after heat treatment at 650 °C for 150 h.

X-ray CT is a nondestructive testing method and can realize the online analysis without destroying the joint. Fig. 8 shows the nano-CT scanning images of the NbTi-Nb_3Sn joint. Fig. 8a indicates the cross section of the joint, which is obtained by scanning the plane where welding spots (spot A) is located. The Nb_3Sn bulk below the figure is prepared by sintering the bulk including the Nb_3Sn wires and the mechanically alloyed precursors at 650 °C for 150 h. NbTi filaments, extruded from the NbTi superconducting wires, are welded together with the Nb_3Sn bulk through resistive welding technology. Six spots are welded along the longitude of the NbTi filaments (A to F).

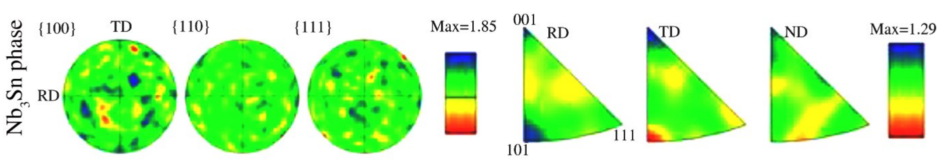

Fig.5 Pole figures and inverse pole figures of the sample

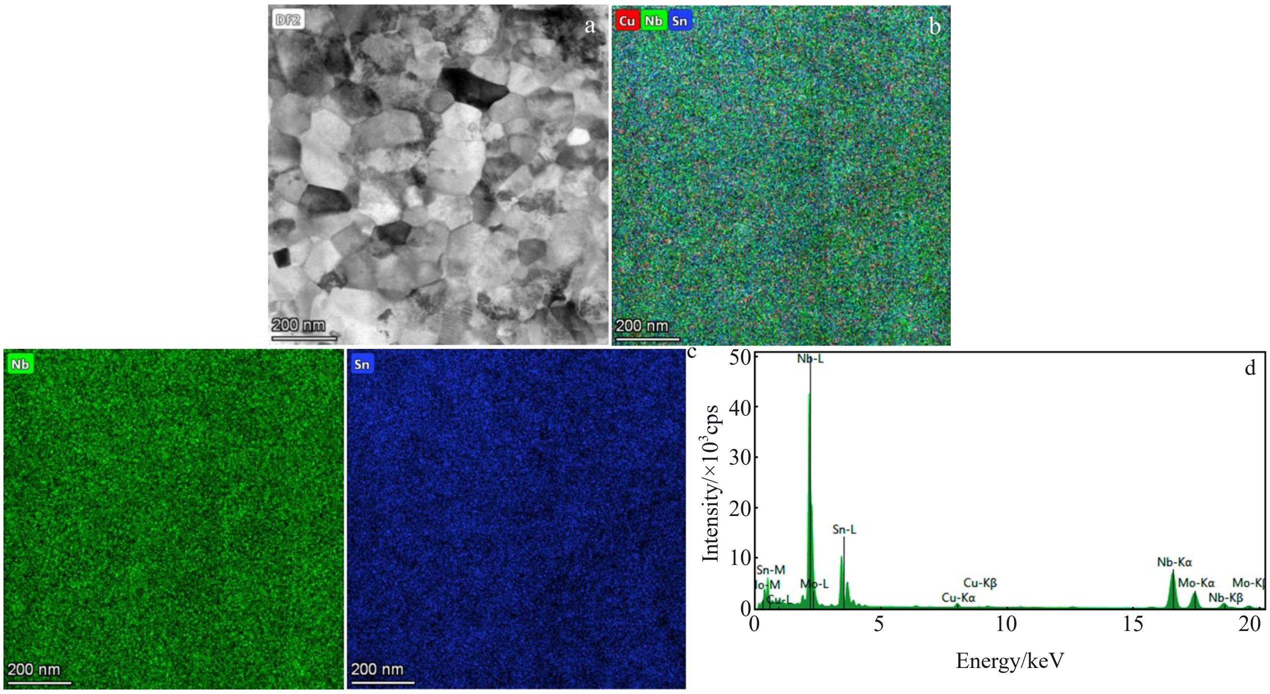

Fig.6 TEM results of the sample heat treated at 650 °C for 150 h: (a) TEM image of Nb_3Sn grains; (b) TEM image and EDS map of Cu, Nb and Sn overlays; (c) EDS mappings of Nb and Sn; (d) EDS spectrum of the sample surface

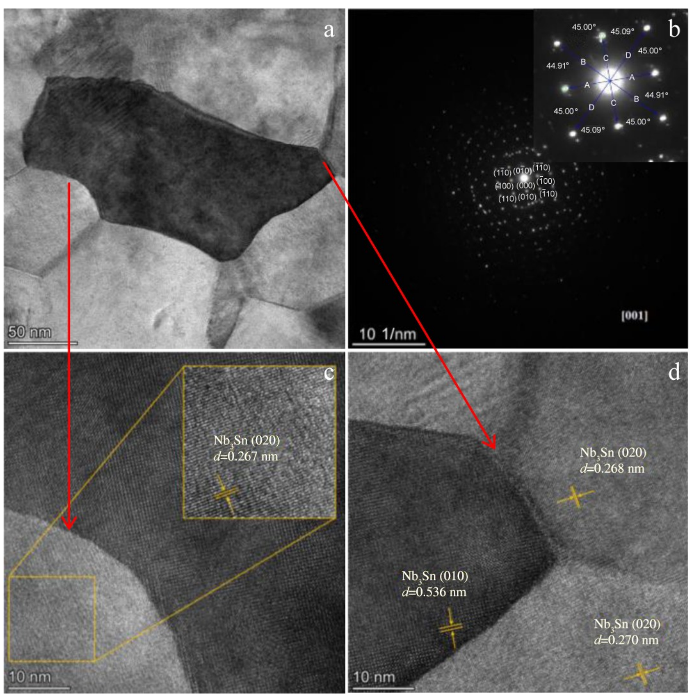

Fig.7 TEM results of Nb_3Sn grains heat treated at 650 °C for 150 h: (a) TEM image, (b) SAED pattern, and (c–d) HRTEM images

Fig.9 shows the nano-CT scanning images of welding spots of the NbTi-Nb_3Sn joint. Fig. 9a shows the longitudinal sectional view, along which three spots are distributed (spot A to C), as shown in the inset of Fig. 9a. The NbTi filaments are welded together with Nb_3Sn within the jointure region. As shown in Fig. 9a, the thickness of NbTi layer significantly declines in the welding spot position. In contrast, the filaments away from the welding spots are loosely arranged. The interfaces between NbTi and Nb_3Sn become blurry. The results confirm that these dissimilar materials are welded together. However, an obvious crack is seen around spot D in the Nb_3Sn bulk, which is a frequent defect in welding. The formation of cracks results in the degradation of the joint strength and electrical properties. Various factors influence the

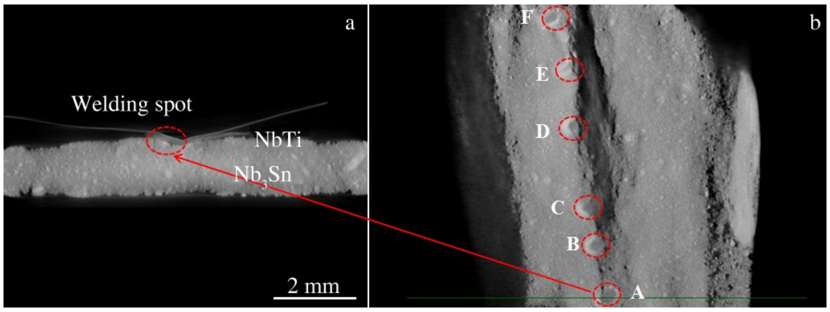

Fig.8 Nano-CT scanning images of cross section (a) and six spots (b) for NbTi-Nb_3Sn joint

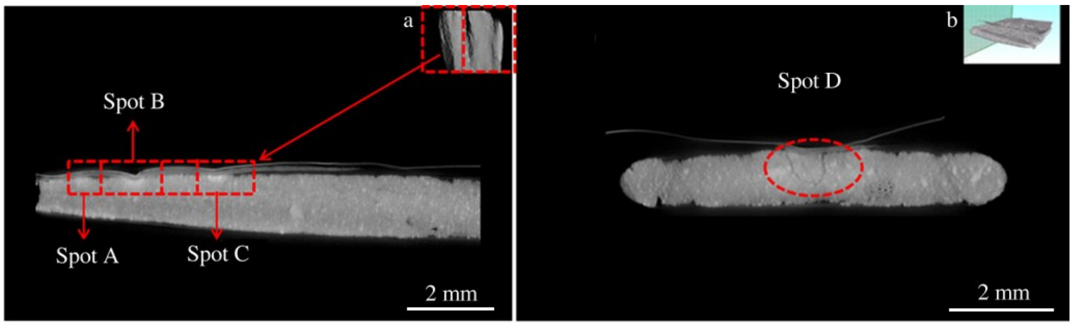

Fig.9 Nano-CT scanning images of welding spots of longitudinal section (a) and obvious crack (b) for the NbTi-Nb_3Sn joint

welding, such as current, cooling rate, and specimen's surface state. The brittleness of Nb_3Sn increases the difficulty of the welding. The cracks appear inside the Nb_3Sn bulk and below the NbTi filaments, thereby enhancing the difficulty of identification. The optimization requires further investigation.

The joint resistance of Nb_3Sn and NbTi was measured at 4.2 K under 1.5 T background field. The joint loop was charged to 100 A using a superconducting powder supply. Fig. 10 shows the decay curve of the magnetic field produced by the current in the closed loop under 1.5 T background field. The joint resistance is 1.3×10^{-13} Ω under 1.5 T background field. The measuring time is approximately 10 h. The joint resistance is barely affected by the magnetic field at 1.5 T. The joint has an advantage over the superconducting solders whose application range is only lower than 0.5 T background field[8]. The process

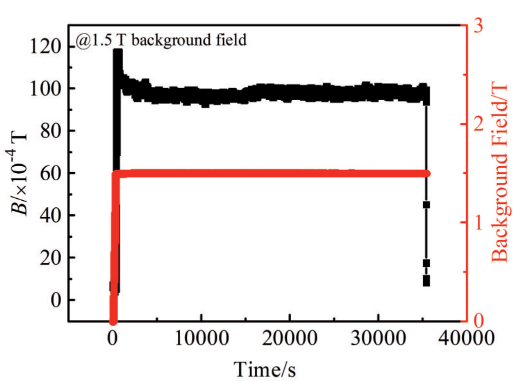

Fig.10 Magnetic field variation in the closed loop against time under 1.5 T background field

does not introduce the extra substance into the joint, and Nb_3Sn material can be connected directly with NbTi material, which allows the Nb_3Sn-NbTi joint to have better magnetic field resistance.

3 Conclusions

1) Superconducting joints between Nb_3Sn and NbTi conductors can be fabricated by the resistive welding technology. The Nb_3Sn joints are first synthesized by sintering the Nb-Sn precursors after mechanical alloying.

2) The Nb_3Sn joints have small grain sizes without excessive growth after long periods of time at high temperature. The Nb_3Sn joint is successfully welded together with the NbTi conductor, although several cracks appear below one spot in Nb_3Sn.

3) The joint of Nb_3Sn and NbTi has ultra-low resistances of 1.3×10^{-13} Ω under 1.5 T background fields, indicating that the joint exhibits better magnetic field resistance compared with the joint fabricated by superconducting solders.

References

1 Godeke A. *Superconductor Science and Technology*[J], 2006, 19: 68

2 Xu Xingchen. *Superconductor Science and Technology*[J], 2017, 30(9): 93 001

3 Baig T, Yao Z, Doll D *et al. Superconductor Science and Technology*[J], 2014, 27(12): 125 012

4 Godeke A, Hellman F, Ten Kate H H J *et al. Superconductor Science and Technology*[J], 2018, 31(10): 105 011

5 Cheng J, Liu J, Ni Z *et al*. *IEEE Transactions on Applied Superconductivity*[J], 2012, 22(2): 43 002
6 Liu J, Cheng J, Zhou F *et al. Cryogenics*[J], 2013, 58: 62
7 Cheng J, Li L, Feng Z *et al. IEEE Transactions on Applied Superconductivity*[J], 2014, 25(3): 4 300 704
8 Cheng J, Wang Q, Feng Z *et al. IEEE Transactions on Applied Superconductivity*[J], 2016, 26(7): 1
9 Hafstrom J W, Killpatrick D H, Niemann R C *et al. IEEE Transactions on Magnetics*[J], 2003, 13(1): 94
10 Sun W, Cheng J, Chen S. *Journal of Low Temperature Physics*[J], 2021, 205: 100
11 Godeke A, Jewell M C, Fischer C M *et al. Journal of Applied Physics*[J], 2005, 97(9): 4545
12 Da Silva L B S, Rodrigues C A, Oliveira Jr N F *et al. Superconductor Science and Technology*[J], 2010, 23(11): 115 012

电阻焊接技术制备Nb_3Sn-NbTi混合超导接头

孙万硕[1,2]，程军胜[1,2,3]，王　磊[1,2,3]，陈顺中[1,2]，郭　强[4]
(1. 中国科学院电工研究所，北京 100190)
(2. 中国科学院大学，北京 100049)
(3. 齐鲁中科电工先进电磁驱动技术研究院，山东 济南 250102)
(4. 西部超导材料科技股份有限公司，陕西 西安 710018)

摘　要：在强磁场超导磁体应用中，特别是具有高稳定度高场超导磁体，具有极低电阻的超导接头发挥着重要作用。通过电阻焊接方法制备了Nb_3Sn和NbTi的异种材料超导接头。首先通过烧结法制备了Nb_3Sn的超导接头，然后通过电阻焊接将Nb_3Sn超导接头与NbTi超导体焊接成型。分析了Nb_3Sn超导接头制备过程中Nb_3Sn的微观组织结构和相变。利用无损检测CT对接头结构进行三维重构，分析了Nb_3Sn和NbTi超导接头内部的缺陷和2种不同材料间的微观连接状态。最后，在背景磁场下对超导接头的电阻性能进行了测试和研究。结果表明，与传统超导焊料制备的超导接头相比，电阻焊接制备的超导接头显示出良好的耐磁场性能，在1.5 T背景磁场下具有较低的电阻值。

关键词：Nb_3Sn超导体；NbTi超导体；超导接头

作者简介：孙万硕，男，1989年生，博士生，中国科学院电工研究所，北京 100190，电话：010-82547259，E-mail：sunwanshuo@mail.iee.ac.cn